

## Grazing incidence X-ray standing wave : a novel technique for measuring ultrasmall diffusion coefficients in polymers

S Dev(nee Sen)\* and B N Dev\*\*

Institute of Physics, Sachivalaya Marg, Bhubaneswar-751 005, India

Received 11 November 1995, accepted 16 November 1995

**Abstract** : The grazing incidence X-ray standing wave technique has recently been used to locate heavy ions in a Langmuir-Blodgett multilayer with a precision of 2 Å. In this communication, we show how this technique can be used for measuring ultrasmall diffusion coefficients ( $\sim 10^{-21}$  cm<sup>2</sup>/sec) in thin polymer films into which a slowly diffusing species has been introduced.

**Keywords** : X-ray standing waves, diffusion in polymers

**PACS Nos.** : 07 85 Yk, 61 41 +e, 68 35 Fx

### 1. Introduction

Thin polymer films on solid surfaces are of great importance in technology due to their wide variety of applications. Diffusion in such polymeric materials is even more important because of various applications ranging from development of photoresists for very large scale integrated (VLSI) circuit fabrication to the performance of membranes for separation processes.

A large number of methods, *e.g.* weight gain [1], transient permeation [2], nuclear magnetic resonance [3], radioactive tracing [4], *etc.* are available for measuring diffusion. Almost all of these measurements do not sense directly the concentration gradient of the diffusing species making it difficult to extract meaningful information from systems which exhibit non-Fickian behaviour. Non-Fickian behaviour is common for many polymer systems [5]. Among other methods used, are scanning infrared microdensitometry

\* Present address : European Molecular Biology Laboratory, EMBL C/o DESY, Notkestrasse 85, 22603 Hamburg, Germany

\*\* Present address : HASYLAB at DESY, Notkestrasse 85, 22603 Hamburg, Germany.

technique [6], electron microprobe techniques [7], radiation damage method [8] *etc.* These methods are destructive. Another good technique is the ion-beam technique or rather the Rutherford backscattering spectrometry (RBS) technique which is well suited for slowly diffusing species. With the RBS technique concentration profiles of the diffusing species are measured with submicrometer depth resolution [9]. However, we will show that by exploiting the subnanometer depth resolution of the grazing incidence X-ray standing wave (XSW) technique, one can measure ultrasmall diffusion coefficients  $D \sim 10^{-21}$  cm<sup>2</sup>/sec. This non-destructive technique can be used in measuring the concentration profiles of small molecules which diffuse slowly into polymers.

## 2. X-ray standing waves

An X-ray standing wave can be generated by causing interference between two coherently related X-ray beams. Conventional X-ray standing wave measurements use dynamical Bragg diffraction [10] from nearly perfect single crystals for generating X-ray standing wave probes with a periodicity around 1–4 Å. This technique was applied to study the lattice location of impurity atoms in crystals with a precision of  $\sim 0.02$  Å [11–13]. It reached a new level of interest when it was realized that the standing wave extends above the surface of the crystal in which it is generated and therefore, could be used for examining adsorbed layers on crystal surfaces [14–17].

X-ray standing waves with a variable period (usually long), can be generated using total external reflection of a monochromatic X-ray beam from a mirror-polished surface. By generating X-ray standing waves above a gold mirror surface, Bedzyk *et al* [18] located a zinc ion layer, which was embedded  $\approx 200$  Å above the mirror surface in a Langmuir-Blodgett multilayer, with a precision of 2 Å.

### *Grazing incidence X-ray standing waves :*

For X-rays the (real part of) index of refraction of any solid or liquid medium is less than unity. Thus, it is possible to obtain total external reflection when an X-ray beam is incident

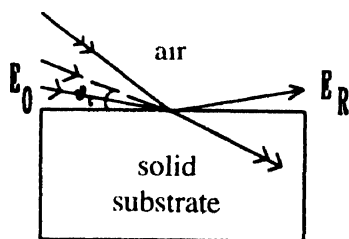


**Figure 1.** Schematic diagram showing total external reflection when the angle of incidence is less than the critical angle  $\theta_c$ .  $E_0$  and  $E_R$  represent the wave amplitudes of the incident and the reflected beam respectively.

on the sample surface at a grazing angle of incidence ( $\theta$ ) less than the critical angle  $\theta_c$  (Figure 1).

The refractive index of the material is in general complex and is given by

$$n = 1 - \delta - i\beta. \quad (1)$$

In eq. (1),  $\delta = r_e \lambda^2 N / 2\pi$  and  $\beta = \lambda \mu / 4\pi$ , where  $r_e$  is the classical electron radius,  $\lambda$  is the wavelength of the incident X-rays,  $N$  is the total number of electrons per unit volume and  $\mu$  is the linear absorption coefficient [19].

Let us consider the case of  $\sigma$ -polarization, *i.e.*, the electric field vectors  $E_0$  and  $E_R$ , associated with the incident and the reflected beam respectively, are perpendicular to the scattering plane. The wave-amplitude ratio for the vacuum/solid interface can be obtained from Fresnel coefficient of reflection [20].

$$\frac{E_R}{E_0} = E_0 e^{i\nu} = \frac{\theta - (\theta^2 - 2\delta - 2i\beta)^{1/2}}{\theta + (\theta^2 - 2\delta - 2i\beta)^{1/2}} \quad (2)$$

where  $\nu$  is the phase of the complex  $E$ -field ratio  $E_R/E_0$ . The reflectivity  $R(\theta)$  is given by

$$R(\theta) = \frac{|E_R|^2}{|E_0|^2} \quad (3)$$

The interference between the two (the incident and the reflected) coherent travelling plane waves generates a standing wave, the electric-field intensity of which at a distance  $z$  from the surface into vacuum is given by [18]

$$I(\theta, z) = |E_0|^2 [1 + R + 2\sqrt{R} \cos(\nu - 2\pi Qz)], \quad (4)$$

where  $Q = 2 \sin \theta / \lambda$ .  $D = 1/Q$  is the periodicity of the standing wave and thus depends on  $\theta$ , the grazing angle of incidence (Figure 1). For  $\theta = \theta_c$  ( $\sin \theta_c \approx \theta_c$ , since  $\theta_c$  is very small) the critical period is

$$D_c = \frac{\lambda}{2\theta_c} = (\sqrt{\pi}/2) [N_a r_e (Z + f')]^{1/2}, \quad (5)$$

where  $r_e$  is the classical electron radius,  $N_a$ ,  $Z$  and  $f'$  are atomic density, atomic number and anomalous dispersion correction for the material of the reflecting surface respectively. For  $f' = 0$ ,  $D_c$  is an energy independent parameter, which is 200 Å for silicon. That is at  $\theta = \theta_c$  for a silicon surface, the antinodes extend outward from the surface with a periodicity of 200 Å. As the angle of incidence increases from zero towards  $\theta_c$ , the positions of the antinodes as well as their periodicity changes. These properties can be exploited to determine the depth distribution of heavy atoms (or molecules containing heavy atoms) confined in a thin film of very low- $Z$  elements (say, a polymer film) on the reflecting surface of a medium or high- $Z$  substrate material. When the embedded heavy atoms are at a given height from the substrate surface, the height can be determined as follows. X-rays will cause photoelectric effect, the cross section of which is proportional to the intensity of X-rays at the centre of an atom (in the dipole approximation). Fluorescence follows the ejection of a photoelectron. Thus by measuring the fluorescence yield, the X-ray ( $E$ -field) intensity on the atom can be estimated. By varying the positions of antinodes above the substrate surface through the variation of  $\theta$ , one can determine when the antinodes have

passed through the atomic layer. The intensity variation of the fluorescence yield as a function of  $\theta$  contains the information about the height of the fluorescing atoms from the substrate surface. If the fluorescing atoms have a concentration distribution, contribution from the concentration at each height will add up to provide an effective fluorescence yield profile. From the analysis of this profile, the concentration distribution can be extracted.

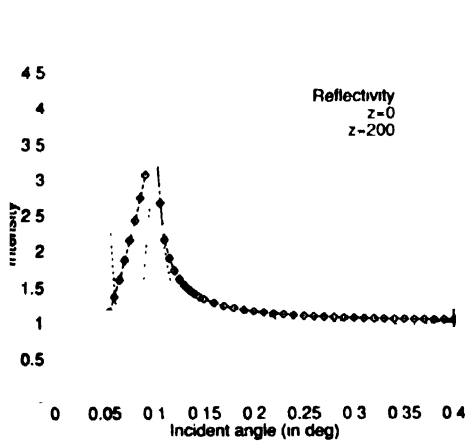


**Figure 2.** Reflectivity and  $E$ -field intensities on the surface ( $z = 0$ ) and at  $200 \text{ \AA}$  above the surface of a silicon substrate

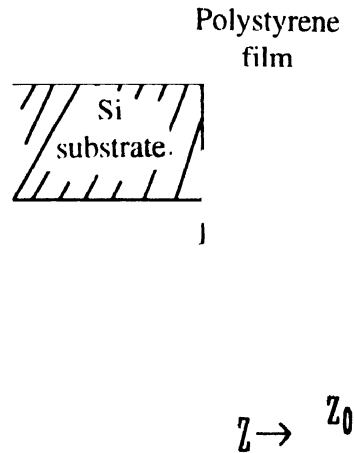


**Figure 3.** A polystyrene thin film of thickness  $z_0$  on a silicon substrate. Before diffusion all absorbed molecules are at  $z_0$ . After diffusion into the film depth distribution of molecules are shown by a half-Gaussian of standard deviation  $\sigma$

Figure 2 shows the reflectivity and the field intensities at  $z = 0 \text{ \AA}$  and  $z = 200 \text{ \AA}$  for a silicon substrate surface. These would be the measured fluorescence yield profile from an atomic or molecular layer on the substrate surface ( $z = 0$ ), and at a height of  $200 \text{ \AA}$ , respectively. The results presented in Figure 2 are for  $\lambda = 0.709 \text{ \AA}$  (Mo  $K_{\alpha 1}$  X-rays :  $17.479 \text{ keV}$ ). Here we will restrict to this value of  $\lambda$  for all calculations. Photons of this energy are suitable for causing  $K$ -fluorescence upto medium- $Z$  atoms and  $L$ -fluorescence in heavier atoms.

### 3. Determination of diffusion coefficients

Let us take a simple model, where a thin polystyrene film is deposited on a silicon surface. The polystyrene film is exposed to bromine vapour to adsorb a molecular (or atomic) layer of bromine. Then, we let these bromine molecules diffuse into the film at a given temperature for a given duration of time. We represent the concentration distribution of bromine by a delta function before diffusion and a half-Gaussian after the diffusion has taken place (Figure 3).

The second distribution is given by

$$G(z) = \tag{6}$$

where  $\sigma$  is the standard deviation. The factor 2 in the numerator of eq. (6) is to ensure that all the molecules are contained in this half-Gaussian;  $z_0$  represents the thickness of the polymer film on top of which the initial  $\delta$ -function-like distribution is located.

Eq. (4) provides the X-ray intensity at a distance  $z$  as a function of the angle of incidence. For the distribution in eq. (6) the intensity is

$$I(\theta) = \int_0^{z_0} I(\theta, z) G(z) dz. \quad (7)$$

We explore the behaviour of  $I(\theta)$  for a specific case : a 200 Å polystyrene film deposited on a mirror-polished silicon substrate; a monolayer film of molecular bromine is then deposited on the surface of the polymer layer.  $I(\theta)$ , the X-ray intensity, or the bromine  $K_{\alpha}$  fluorescence yield for this case, is shown in Figure 4.

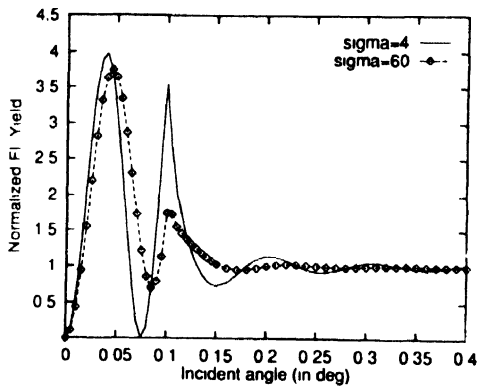


Figure 4. The X-ray intensity  $I(\theta)$  or the fluorescence yield as a function of  $\theta$  for the distribution in eq. (6) and Figure 3

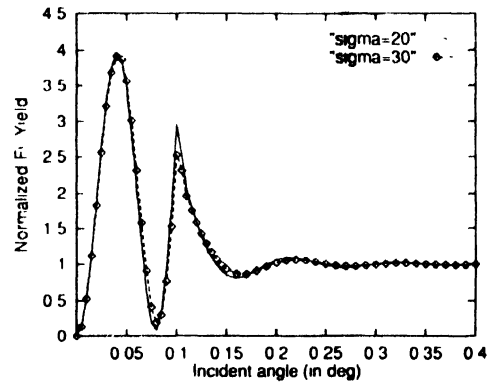


Figure 5.  $I(\theta)$  vs  $\theta$  plot for two values of  $\sigma$  differing by 10 Å. Changes in peak (or dip) positions as well as in intensity modulation are easily distinguishable

Prior to diffusion, the bromine distribution should realistically be a Gaussian (rather than a delta function) because the polymer surface on which bromine is deposited would certainly have a surface roughness, some of which might arise from the roughness of the silicon surface on which the polymer film is deposited. The smallest roughness expected is of the order of a few angstrom [21]. That is why we have actually evaluated  $I(\theta)$  for a Gaussian with  $\sigma = 4$  Å. The diffused profile corresponds to  $\sigma = 60$  Å. It is seen from the figure (Figure 4) that the fluorescence yield profiles are drastically different.

Figure 5 shows  $I(\theta)$  for two different  $\sigma$  values (20 Å and 30 Å) differing by 10 Å. It is clear that the two curves are distinguishable in intensity as well as peak (or dip) position shifts. A larger value of  $\sigma$  brings more bromine molecules closer to the silicon surface. Thus, more molecules see the antinodes at slightly larger  $\theta$ . It may be noted that when the fluorescing atoms are at the substrate surface ( $z = 0$ ), they do not see an antinode until  $\theta = \theta_c$  is reached. This is evident from the peak in the  $I(\theta)$  vs  $\theta$  curve in Figure 2.

Noting that, in the Fickian solution to the diffusion problem,  $\sigma \approx (Dt)^{1/2}$ , where  $D$  is the diffusion coefficient and  $t$  is the time duration over which the diffusion process has

occurred, we can estimate the smallest order of magnitude of  $D$  that can be measured using the grazing incidence X-ray standing wave technique. As shown in Figure 5, a  $(Dt)^{1/2}$  value of  $10 \text{ \AA}$  is easily measurable. It may be noted that the technique has a position resolution of  $\sim 2 \text{ \AA}$  [18]. First, how large a  $t$  is practicable? Romanelli *et al* [9] studied iodine diffusion in polymer (polyimide) by Rutherford backscattering spectrometry (RBS). They used a diffusion time of 19 days. They estimated that for a diffusion time of one month a  $D$ -value of about  $10^{-17} \text{ cm}^2/\text{sec}$  could be measured by the RBS technique. With the grazing incidence XSW technique  $t = 1 \text{ month}$  ( $\sim 2.6 \times 10^6 \text{ sec}$ ) would enable one to measure a  $D$  as small as  $10^{-21} \text{ cm}^2/\text{sec}$  [ $(Dt)^{1/2} = 10 \text{ \AA}$ ,  $D = 3.8 \times 10^{-21} \text{ cm}^2/\text{sec}$ ].

The particular case we have discussed here, may not give rise to exactly a half-Gaussian profile after diffusion has occurred. However, it does not affect the points of our discussion. If another layer of polymer is deposited above the bromine layer, this situation may be described as diffusion into a semi-infinite solid from a thin planar source. The solution to this problem is known [22] and the concentration profile of bromine would be a full Gaussian spreading symmetrically outwards from the initial position with  $\sigma = (2Dt)^{1/2}$ . In this situation, unlike Figure 4, the peak positions in the  $I(\theta)$  vs  $\theta$  plot would not shift, only the modulation will be reduced as shown in Figure 6. Again a change of  $\sigma = 10 \text{ \AA}$  can

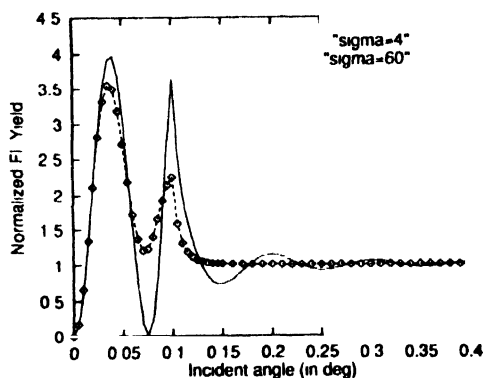


Figure 6.  $I(\theta)$  vs  $\theta$  plot for the case of diffusion into a semi-infinite film from a thin planar source

be easily measured. When diffusion process is allowed to proceed while the polymer surface is kept exposed to bromine, the concentration profile would be a complementary error function, for which  $I(\theta)$  can be calculated and measured with the same precision. In this case also, like Figure 4 for a larger value of  $\sigma$  (*i.e.*, long exposure time for constant  $D$ ), the peaks in the  $I(\theta)$  plot would shift towards larger  $\theta$  in addition to a reduction in modulation. In all the cases, experimental data could be fitted to the theoretical models to extract the diffusion coefficients, and also detect possible deviations from Fickian behaviour.

For a thicker polymer layer, say  $1000 \text{ \AA}$  ( $= 5 D_c$ ) about five complete peaks would be observed in the  $I(\theta)$  vs  $\theta$  curve. The general arguments about peak position shifts and

modulation changes discussed above for the case of the 200 Å film will still be applicable. As the film thickness increases, the number of peaks also increases and the largest usable thickness will be dictated by the precision with which  $\theta$  can be measured.

In computing the contents of Figures 4, 5 and 6, we have actually neglected the presence of the polymer layer as it is composed of low- $Z$  elements, *e.g.* C and H, and thus a weak scatterer. This layer can be explicitly included in the computation [20]. However, it would not bring any significant change in the results presented here.

#### 4. Conclusions

In this paper, we have proposed a method based on grazing incidence X-ray standing waves for the determination of ultrasmall ( $\sim 10^{-21}$  cm<sup>2</sup>/sec) diffusion coefficients in polymer films. It would not be difficult to perform experiments on the specific systems used as examples in this paper.

#### References

- [1] S Prager and F A Long *J Am Chem Soc* **73** 4072 (1951)
- [2] J Crank and G S Park *Diffusion in Polymers* (New York) (1968)
- [3] V J Mc Brierty and D C Douglas *Phys Rep* **63** 61 (1980)
- [4] Y Kumagai, H Wanabe, K Miyasaka and T Hata *J Chem. Engg Jpn* **12** 1 (1979)
- [5] T Alfrey, E F Gurney and W G Lloyd *J Polym Sci* **C12** 249 (1966)
- [6] J Klein and B J Briscoe *Proc Roy Soc London* **A365** 53 (1979)
- [7] P T Gilmore, R Falabella and R L Lawrence *Macromolecules* **13** 880 (1980)
- [8] T Venkatesan, D Edelson and W L Brown *Appl Phys Lett.* **43** 364 (1983)
- [9] J F Romanelli, J W Mayer and E J Kramer *J Polymer Sci Polymer Phys edn* **24** 263 (1986)
- [10] B W Battermann and H Cole *Rev Mod Phys.* **36** 681 (1964)
- [11] B W Battermann *Phys. Rev.* **133** A759 (1964)
- [12] J A Golovchenko, B W Battermann and W L Brown *Phys Rev* **B10** 4239 (1974)
- [13] S K Andersen, J A Golovchenko and G Mair *Phys Rev Lett.* **37** 1141 (1976)
- [14] P L Cowan, J A Golovchenko and M F Robbins *Phys. Rev. Lett* **44** 1680 (1980)
- [15] J A Golovchenko, J R Patel, D R Kaplan, P L Cowan and M J Bedzyk *Phys Rev. Lett.* **49** 560 (1982)
- [16] B N Dev, G Materlik, F Grey, R L Johnson and M Clausnitzer *Phys Rev Lett* **57** 3058 (1986)
- [17] J Zegenhagen *Surf Sci. Rep.* **18** 199 (1993)
- [18] M J Bedzyk, G M Bommarito and J S Schildkraut *Phys. Rev. Lett* **62** 1376 (1989)
- [19] R W James *The Optical Principles of Diffraction of X-rays* (Woodridge : Ox Bow) Ch 13 (1982)
- [20] L G Parrat *Phys. Rev.* **95** 359 (1954)
- [21] P V Satyam, D Bahr, S K Ghose, G Kuri, B Sundaravel, B Rout and B N Dev *Curr. Sci (India)* **69** 526 (1995)
- [22] R J Borg and G J Dienes *An Introduction to Solid State Diffusion* (New York Academic) Ch 1 (1988)